Smart Grid and Renewable Energy, 2025, 16(6), 111-130
https://www.scirp.org/journal/sgre
ISSN Online: 2151-4844
ISSN Print: 2151-481X

Numerical and Experimental Study of a Continuous Refrigeration Production System by Adsorption

Amadou Diallo[1], Adama Ouedraogo[2*], Hassime Guengane[3], Wende Pouiré Germain Ouedraogo[4], Amadou Konfé[1], Sié Kam[1], Dieudonné Joseph Bathiebo[1]

[1]Thermal Energy and Renewable Energy Laboratory, Joseph KI ZERBO University, Ouagadougou, Burkina Faso
[2]Kaya Polytechnic University Center, Kaya, Burkina Faso
[3]Ecole Polytechnique de Ouagadougou, Ouagadougou, Burkina Faso
[4]4th District of the University of Toguyeni, Fada N'Gourma, Burkina Faso
Email: *adama1.ouedraogo@ujkz.bf

How to cite this paper: Diallo, A., Ouedraogo, A., Guengane, H., Ouedraogo, W.P.G., Konfé, A., Kam, S. and Bathiebo, D.J. (2025) Numerical and Experimental Study of a Continuous Refrigeration Production System by Adsorption. *Smart Grid and Renewable Energy*, **16**, 111-130.
https://doi.org/10.4236/sgre.2025.166007

Received: June 11, 2025
Accepted: June 27, 2025
Published: June 30, 2025

Abstract

This work focuses on the design, modeling and numerical simulation of a solar adsorption refrigeration system. The model studied is powered by solar thermal energy and uses the silica gel/water pair. The objective is to carry out a thermodynamic study of the adsorption system coupled to a cold room. The advantage of this device is that it uses a torque that is not harmless to the environment, without noise pollution, a technology that is easy to achieve. The modeling of the system is carried out with the TRNSYS software, and an experimental validation is carried out on the LESBAT platform. The climatic input parameters for the simulation are those of the city of Ouagadougou to approximate the real operating conditions of the system. We present the temperature variation of the prototype of continuous refrigeration production by adsorption. Thus, the solar performance factor (COP) and the cooling capacity (SCP) are the parameters studied to evaluate the performance of the system. For a mass of 22 kg of silica gel, a temperature of the heat sink or condenser Tc of 25˚C and a hot source temperature of 90˚C, we obtained a COP of about 0.7 and an SCP of 200 W/kg.

Keywords

Adsorption, Silica Gel/Water, Experimental Study, TRNSYS, Coefficient of Thermal Performance, Cooling Capacity

1. Introduction

In Burkina Faso, as in many developing countries, the demand for refrigeration

for food preservation is increasing [1]. For example, the dairy sector in Burkina Faso is facing major challenges related to losses. The dairy sector is mainly made up of small farmers and breeders, operating in often precarious conditions in terms of milk storage and processing infrastructure [2]. Rural populations residing outside the areas covered by the electricity grid do not have access to refrigeration systems. In addition, the energy supplied by the National Electricity Company of Burkina Faso (SONABEL) is mainly of fossil origin and conventional compression refrigerators use refrigerants that are very harmful to the environment [3].

In this context, and particularly in countries with abundant sunshine, the use of solar energy for cold production appears to be a promising solution. Sorption solar systems can be a sustainable solution for these problems because they are adapted to the specific climatic conditions of Burkina Faso. Despite intermittent refrigeration, these systems offer a key advantage in the simplicity of their design (eliminating the need for spare parts or mechanical interventions) and complete energy autonomy during the refrigeration production phase. In addition, this technology has a low impact on the environment.

The system envisaged in this study uses the adsorption phenomenon, silica gel as an adsorbent, water as a refrigerant and solar energy as an energy source. These machines operate with two pressure levels: high pressure in the generator and condenser and low pressure in the evaporator and adsorber.

Several designs of adsorption refrigeration systems have been studied in the literature, of which a few examples can be cited.

Bidyut *et al.* [4] use a two-element adsorption cooling system with silica gel as the adsorbent and water as the adsorbat. The numerical study by Leong *et al.* [5] of a refrigeration system with two adsorption beds with heat and mass recovery showed the effects of bed dimensions, bed thermal conductivity, heat transfer fluid flow, generation temperature and heat recovery on system performance. Hamamoto *et al.* [6] investigated the cycle performance of a two-bed adsorption cooling system using active carbon fibers (ACF)/methanol as an adsorbent/adsorbate pair. Alam *et al.* [7] designed and studied a two-stage four-stage adsorption bed cooling system with the silica gel-water pair. Nidal *et al.* [8] presented a new design of a solar adsorption refrigeration unit that is composed of four adsorbent beds with different types of activated carbon (jojoba seeds, palm seeds, coconut, and activated carbon). Ruud *et al.* [9] designed and experimentally studied an adsorption cooling system with the silica gel-water pair.

Our work aims to meet the needs of food preservation in non-electrified rural areas of Burkina Faso, while maximizing thermodynamic performance and minimizing environmental impact through a solar adsorption refrigeration system using the silica gel/water couple.

The system studied in this work is composed of two beds of identical adsorbents, operating in phase opposition in order to ensure the continuous production of cold.

In this paper, we study the key parameters of the two-bed adsorption refrigeration system operating under the climatic conditions of Burkina Faso. The study of these parameters will make it possible to identify the optimal conditions for refrigeration production when the system is coupled with cold rooms and air distribution units for air conditioning needs.

2. Materials and Methods

In this study, we use the simulation tool TRNSYS17 for system modeling to predict performance and study the operating parameters of the system from a theoretical point of view. A test bench has been developed at the LESBAT laboratory of HEIC-CV for the experimental part.

2.1. TRNSYS Software Overview

TRNSYS software is a highly flexible graphical software environment used to simulate the behavior of transient systems. While the vast majority of simulations focus on evaluating the performance of thermal and electrical power systems, TRNSYS can also be used to model other dynamical systems such as circulation or biological processes.

TRNSYS is made up of two parts. The first part is an engine (called a kernel) that reads and processes the input file, resolves the system iteratively, determines convergence, and plots system variables. The kernel also provides utilities that (among other things) determine thermophysical properties, invert matrices, perform linear regressions, and interpolate external data files. The second part of TRNSYS is an extensive library of components, each of which models the performance of a part of the system. In this study, we therefore propose a refrigeration production system capable of meeting conservation needs.

2.2. Weather Data

In our work, we used meteorological data contained in the TRNSYS software database from SOLARGIS. These data are corroborated by those provided by those provided by the meteorological stations of Burkina Faso. Satellite data have the advantage of being continuous over time with a fine mesh of space. This allows us to easily obtain the data for our study site.

2.3. Description of the Study Site

Ouagadougou is located in the center of the country at an altitude of 300 meters, in the middle of the intertropical zone, with strong sunshine as shown in **Figure 1** [10]. The city has, on average, 3135 hours of sunshine per year. Ouagadougou's climate is tropical, warm all year round, with a dry season from November to March and a rainy season that runs approximately from late April to early October. During the day, it can be very hot all year round, but especially from March to May, before the rainy season. The city has a tropical savannah climate, with two seasons: the harmattan and the monsoon. Cut off from the influence of the

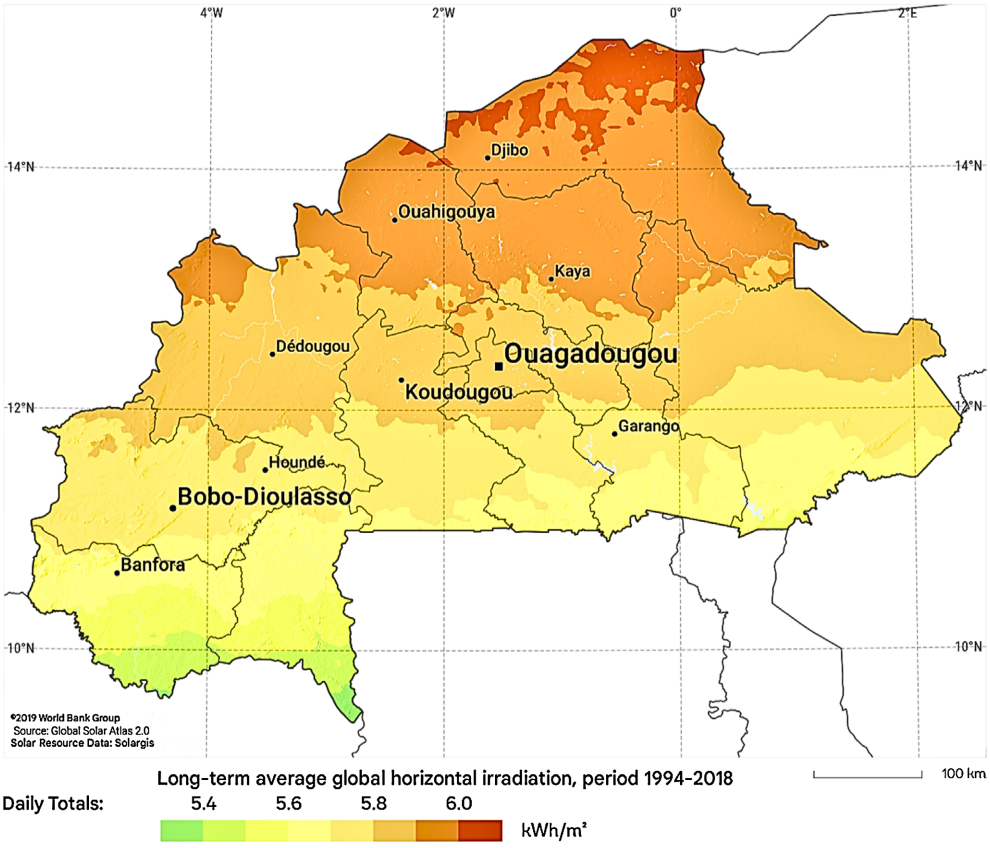

Figure 1. Sunshine Ouagadougou, Burkina Faso [10].

desert and any ventilation, the city then suffered from scorching weather, with scorching days (from 38˚C at the end of February to 40˚C to 42˚C and even 43˚C in April) and hot nights (on average 24˚C to 26˚C at least, with even a few nights when the temperature did not drop below 30˚C in April).

The city has a tropical savannah climate, with two seasons: the harmattan and the monsoon. Cut off from the influence of the desert and any ventilation, the city then suffered from scorching weather, with scorching days (from 38˚C at the end of February to 40˚C to 42˚C and even 43˚C in April) and hot nights (on average 24˚C to 26˚C at least, with even a few nights when the temperature did not drop below 30˚C in April) according to **Figure 2** [11].

3. Description of the System Studied

The continuous adsorption cooling system studied is illustrated in **Figure 3**. The system uses silica gel as an adsorbent and water as a refrigerant and consists essentially of four components: two identical adsorption/desorption beds filled with adsorbent, an evaporator and a condenser [12]. The adsorbent bed is the most essential element of the system, playing the role of a compressor in a compression refrigeration system. The regeneration of silica gel in the bed is carried out by a solar hot water source. The average temperature of the coldest month (January) is 25.4˚C, that of the hottest month (April) is 33.7˚C. One of the flagship

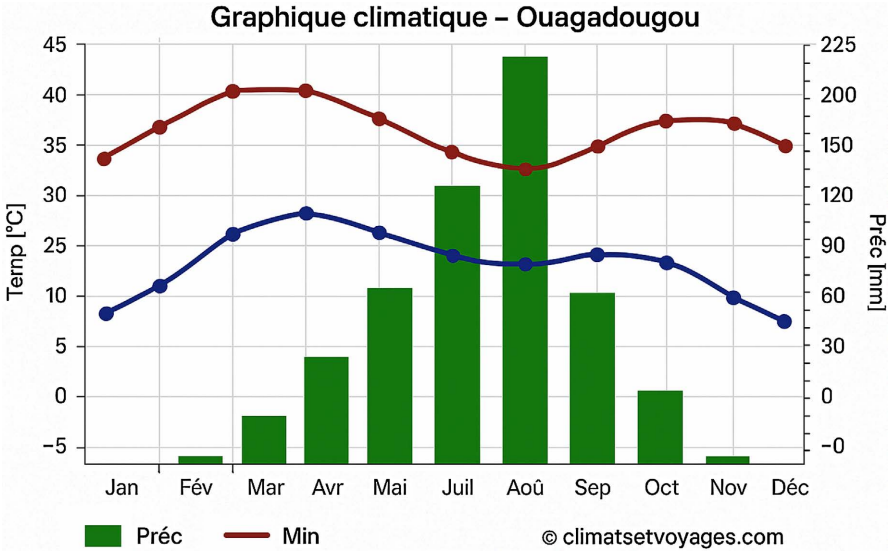

Figure 2. Ombro-thermal diagram of Ouagadougou, 2021 [11].

commercial activities of the populations of the city's outlying districts are the production and marketing of dairy products (yoghurt, gapal, etc.). However, these areas are most often outside the perimeter of the national electricity grid coverage or lack adequate conservation resources.

There is also a high rate of post-harvest loss of agricultural products, mainly due to inadequate means and/or techniques of preservation.

3.1. Working Principle of the Ideal Cycle

The working principle of the adsorption refrigeration system is based on an adsorption-desorption thermal cycle. This cycle can be represented on a Clapeyron diagram on **Figure 3** [13]. It is divided into four phases, namely isosteric heating in phase 1, desorption in phase 2, isosteric cooling in phase 3 and adsorption in phase 4.

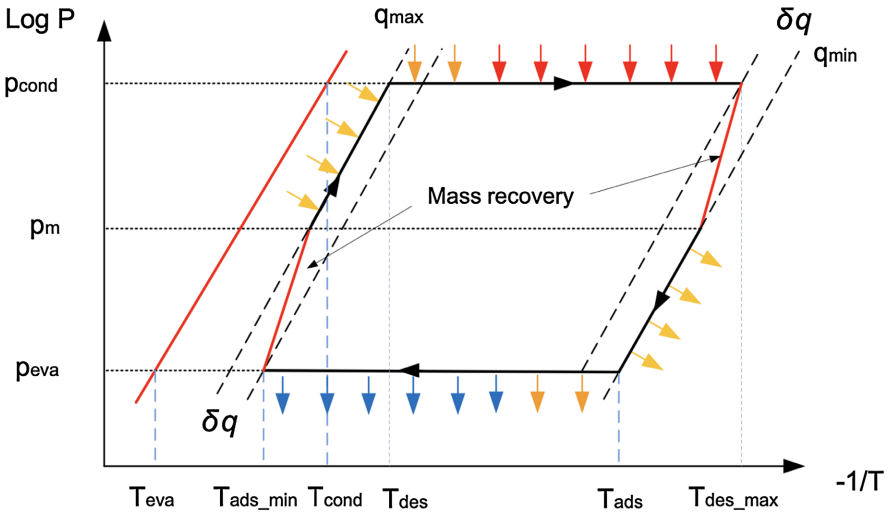

Figure 3. Diagram of the thermal cycle at adsorption/desorption [13].

1) Initially, the adsorption bed is saturated with water vapour and is isolated from the condenser and evaporator using valves. It is heated adsorber until the vapour pressure in the adsorption bed reaches the condensation pressure (Pcd) of the water.

2) At this time, the adsorption bed is connected to the condenser and the desorbed liquid is cooled to a temperature (Tcd) until it condenses in the condenser.

3) Meanwhile, the adsorbent bed is closed, and the adsorbent releases the heat using a cold fluid source. During this cooling phase, the temperature and pressure inside the adsorbent bed decrease.

4) The bed is connected to the evaporator as soon as the bed pressure becomes slightly lower than the evaporation pressure (Pev). As the adsorbent continues to cool, the liquid water vaporized in the evaporator is adsorbed by the adsorbent. This vapor is produced by evaporation of the liquid in the evaporator, thus producing cold. The amount of cold produced is proportional to the latent heat of vaporisation of the adsorbat.

3.2. Principle of Continuous Refrigeration

To ensure the continuity of operation of the cold production by adsorption, we have a second adsorption bed. According to **Figure 3** the operating principle is as follows:

1) During phase 1, the adsorbent of the first compartment (reactor 2) is "regenerated" by heating (hot water from the solar collector).

2) During phase 2, the water vapour produced flows under the influence of a vacuum pushed to the condenser where it is condensed. Thus, the condensed water flows through the expansion valve to the low-pressure evaporator where it is evaporated (low-temperature production step).

3) Then in phase 3, the adsorbent in the second chamber (reactor 1) maintains low pressure by adsorbing water vapor from the evaporator.

4) Finally, wind phase 4, or the compartment, needs to be cooled to maintain the adsorption process.

When the production of cold decreases (the adsorbent becomes saturated with water vapour), the functions of the two compartments are reversed (by opening and closing the valves). For systems with mass recovery, connect the generator (reactor 2) through the valve to the adsorber (reactor 1) in phase 3. The adsorbate is evaporated from the generator and transferred directly to the adsorber until pressure equilibrium is reached [14]. The mass of adsorption and desorption increases, leading to an increase in the cycled mass, which translates into an increase in cold production.

4. Modelling of the System Studied

We used a model that was originally developed for the dynamic simulation of two-bed silica gel water adsorption chillers. The model is based on a flat-parameter modeling approach similar to the work of Wang *et al.* [15]. The main inputs, pa-

rameters and results of the model are presented in Figure 4.

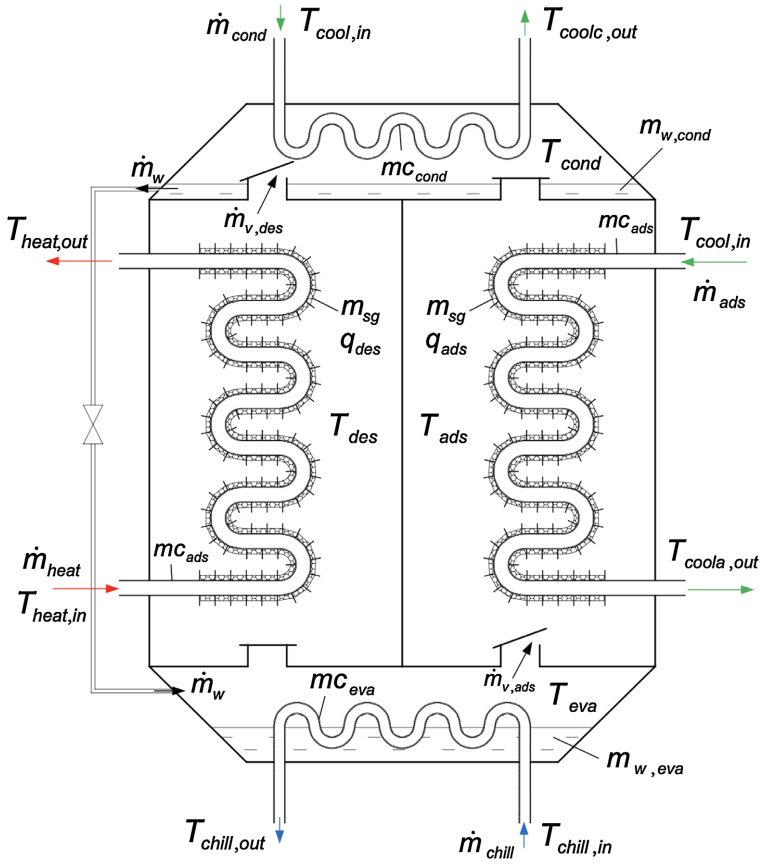

Figure 4. Model of a two-bed desiccant chiller [15].

4.1. Mathematical Modelling of the Operating Cycle

To simplify the equations we have formalized the following information: adsorption/desorption takes place at equilibrium, temperature and pressure are uniform in all chambers, the empty volume of the chambers is neglected, the adsorbent is inert, the thermal mass of the heat transfer fluid is neglected during the adsorption/desorption process, the adsorbed phase is assumed to be a saturated liquid, and the average isosteric adsorption heat is constant [16]. The energy and mass balances for each component of the system are carried out in a non-steady state.

4.2. Equation

The mass balance of the adsorbate during the cycle is expressed in the following equations which describe the principle.

- At the desorber, we have the mass flow of the desorbed water vapour which is given by Equation (1):

$$\dot{m}_{v,des} = -m_{sg} \frac{\mathrm{d}q_{des}}{\mathrm{d}t} \tag{1}$$

- At the level of the condenser, we have:

$$\frac{\mathrm{d}m_{w,cond}}{\mathrm{d}t} = \dot{m}_{v,des} - \dot{m}_{w} \tag{2}$$

- At the evaporator level, we have:

$$\frac{\mathrm{d}m_{w,eva}}{\mathrm{d}t} = \dot{m}_{w} - \dot{m}_{v,ads} \tag{3}$$

- At the adsorber level, we have:

$$m_{sg}\frac{\mathrm{d}q_{ads}}{\mathrm{d}t} = \dot{m}_{v,ads} \tag{4}$$

Define the different terms of Equations (1) to (4).

4.2.1. Thermal Balance

During the adsorption/desorption cycle, neglecting changes in kinetic and potential energy, the first law of thermodynamics allows us to obtain the following equation at the level of:

- first compartment (adsorption/desorption).

$$\begin{aligned}&\left(mc_{p,ads} + m_{sg}\left(c_{p,sg} + c_{p,w}q_{des}\right)\right)\frac{\mathrm{d}T_{des}}{\mathrm{d}t}\\&= \dot{m}_{heat}c_{p,w}\left(T_{heat,in} - T_{heat,out}\right) + \delta\dot{m}_{v,des}\left(h_{v}T_{des} - h_{v}T_{cond}\right) + m_{sg}\frac{\mathrm{d}q_{des}}{\mathrm{d}t}q_{st}\end{aligned} \tag{5}$$

- second compartment (adsorption/desorption).

$$\begin{aligned}&\left(mc_{p,ads} + m_{sg}\left(c_{p,sg} + c_{p,w}q_{ads}\right)\right)\frac{\mathrm{d}T_{ads}}{\mathrm{d}t}\\&= \dot{m}h_{ads}c_{p,w}\left(T_{cool,in} - T_{coola,out}\right) + \left(1-\phi\right)\dot{m}_{v,ads}\left(h_{v}T_{eva} - h_{v}T_{ads}\right) + m_{sg}\frac{\mathrm{d}q_{ads}}{\mathrm{d}t}q_{st}\end{aligned} \tag{6}$$

- condenser we have:

$$\begin{aligned}&\left(mc_{cond} + m_{w,cond}c_{p,w}\right)\frac{\mathrm{d}T_{cond}}{\mathrm{d}t}\\&= \dot{m}_{cond}c_{p,w}\left(T_{cool,in} - T_{cool,out}\right) + \left(1-\delta\right)\dot{m}_{v,des}\left(h_{v}T_{des} - h_{v}T_{cond}\right) + \dot{m}_{v,des}h_{fg}T_{cond}\end{aligned} \tag{7}$$

- At the evaporator level, we have:

$$\begin{aligned}&\left(mc_{p,eva} + m_{w,eva}c_{p,w}\right)\frac{\mathrm{d}T_{eva}}{\mathrm{d}t}\\&= \dot{m}_{chill}c_{p,w}\left(T_{chill,in} - T_{chill,out}\right) - \dot{m}_{v,ads}h_{fg}T_{eva}\\&\quad + \dot{m}_{w}c_{p,w}\left(T_{cond} - T_{eva}\right) + \phi\dot{m}_{v,ads}\left(h_{v}T_{eva} - h_{v}T_{ads}\right)\end{aligned} \tag{8}$$

4.2.2. Heat Exchanges

For the heat transfer of the heat transfer fluid at the level of the first adsorber/desorber, we have:

$$T_{heat,out} = T_{des} + \left(T_{heat,in} - T_{des}\right)\mathrm{e}^{\frac{-UA_{des}}{\dot{m}_{heat}c_{p,w}}} \tag{9}$$

For the heat transfer of the heat transfer fluid at the level of the second adsorber/desorber, we have:

$$T_{coola,out} = T_{ads} + \left(T_{cool,in} - T_{ads}\right) e^{\frac{-UA_{ads}}{\dot{m}_{ads} c_{p,w}}} \tag{10}$$

For the heat transfer of the heat transfer fluid within the condenser, we have:

$$T_{cool,out} = T_{cond} + \left(T_{cool,in} - T_{cond}\right) e^{\frac{-UA_{cond}}{\dot{m}_{cond} c_{p,w}}} \tag{11}$$

For the heat transfer of the heat transfer fluid within the evaporator we have:

$$T_{chill,out} = T_{eva} + \left(T_{chill,in} - T_{eva}\right) e^{\frac{-UA_{eva}}{\dot{m}_{chill} c_{p,w}}} \tag{12}$$

For the heat recovery equation at the level of the first adsorber/desorber, we have:

$$\left(mc_{ads} + m_{sg}\left(c_{p,sg} + c_{p,w} q_{des}\right)\right)\frac{\mathrm{d}T_{des}}{\mathrm{d}t} = \dot{m}_{heat} c_{p,w}\left(T_{heat,in} - T_{heat,out}\right) \tag{13}$$

$$m_w c_{p,heat}\frac{\mathrm{d}\overline{T}_m}{\mathrm{d}t} = \dot{m} c_{p,heat}\left(T_{heat,in} - T_{heat,out}\right) + UA_{des}\left(T_{des} - \overline{T}_m\right) \tag{14}$$

For the heat recovery equation at the level of the second adsorber/desorber, we have:

$$\left(mc_{ads} + m_{sg}\left(c_{p,sg} + c_{p,w} q_{ads}\right)\right)\frac{\mathrm{d}T_{ads}}{\mathrm{d}t} = \dot{m}_{ads} c_{p,w}\left(T_{cool,in} - T_{coola,out}\right) \tag{15}$$

$$m_w c_{p,cool}\frac{\mathrm{d}\overline{T}_m}{\mathrm{d}t} = \dot{m} c_{p,cool}\left(T_{cool,in} - T_{cool,out}\right) + UA_{ads}\left(T_{ads} - \overline{T}_m\right) \tag{16}$$

For the heat recovery equation at the condenser, we have:

$$\left(mc_{cond} + m_{w,cond} c_{p,w}\right)\frac{\mathrm{d}T_{cond}}{\mathrm{d}t} = \dot{m}_{cond} c_{p,w}\left(T_{cool,in} - T_{cool,out}\right) \tag{17}$$

For the heat recovery equation at the evaporator, we have:

$$\left(mc_{eva} + m_{w,eva} c_{p,w}\right)\frac{\mathrm{d}T_{eva}}{\mathrm{d}t} = \dot{m}_{chill} c_{p,w}\left(T_{chill,in} - T_{chill,out}\right) \tag{18}$$

At rest, the heat losses due to the first adsorber/desorber are determined by:

$$\left(mc_{ads} + m_{sg}\left(c_{p,sg} + c_{p,w} q_{des}\right)\right)\frac{\mathrm{d}T_{des}}{\mathrm{d}t} = UA_{des,amb}\left(T_{room} - T_{des}\right) \tag{19}$$

At rest, the heat losses due to the second adsorber/desorber are determined by:

$$\left(mc_{ads} + m_{sg}\left(c_{p,sg} + c_{p,w} q_{ads}\right)\right)\frac{\mathrm{d}T_{ads}}{\mathrm{d}t} = UA_{ads,amb}\left(T_{room} - T_{ads}\right) \tag{20}$$

At rest, heat losses from the condenser are determined by:

$$\left(mc_{cond} + c_{w,\text{ɔond}}\right)\frac{\mathrm{d}T_{cond}}{\mathrm{d}t} = UA_{cond,amb}\left(T_{room} - T_{cond}\right) \tag{21}$$

At rest, heat losses in the evaporator are determined by:

$$\left(mc_{eva} + c_{w,eva}\right)\frac{\mathrm{d}T_{eva}}{\mathrm{d}t} = UA_{eva,amb}\left(T_{room} - T_{eva}\right) \tag{22}$$

4.2.3. Adsorption Equilibrium

The adsorption equilibrium equation is given by:

$$q^* = k_s\left(q^* - q\right) \tag{23}$$

At equilibrium, we have:

$$\frac{\mathrm{d}q}{\mathrm{d}t} = k_s\left(q^* - q\right),\ k_s = \frac{15D_s}{R_p^2} \tag{24}$$

For the recovery of the mass, we have:

$$\begin{aligned}&\left(mc_{ads} + m_{sg}\left(c_{p,sg} + c_{p,w}q_{ads}\right)\right)\frac{\mathrm{d}T_{ads}}{\mathrm{d}t}\\&= m_{sg}\frac{\mathrm{d}q_{ads}}{\mathrm{d}t}q_{st} + m_{sg}\frac{\mathrm{d}q_{ads}}{\mathrm{d}t}\left(h_v T_{des} - h_v T_{ads}\right)\end{aligned} \tag{25}$$

$$\left(mc_{des} + m_{sg}\left(c_{p,sg} + c_{p,w}q_{des}\right)\right)\frac{\mathrm{d}T_{des}}{\mathrm{d}t} = m_{sg}\frac{\mathrm{d}q_{des}}{\mathrm{d}t}q_{st} \tag{26}$$

$$m_{sg}\frac{\mathrm{d}q_{ads}}{\mathrm{d}t} = -m_{sg}\frac{\mathrm{d}q_{des}}{\mathrm{d}t} \tag{27}$$

4.2.4. System Performance Coefficient

Starting from the assumption in which we neglect the energy consumed by the circulators and other accessories, the Coefficient of Performance (COP) is determined by the following formula:

$$COP = \frac{Q_{ev}}{Q_{gn}} \tag{28}$$

Q_{ev} and Q_{gn} are respectively the amount of cold produced at the evaporator and the amount of heat at the hot source.

And the specific cooling power is given by:

$$SCP = \frac{Q_{ev}}{m_{ads}} \tag{29}$$

4.3. Numerical and Experimental System Resolution

To solve the equations of the model, we used the TRNSY software to analyze the influence of the different parameters on the functioning of the studied system.

We also used the test bench for experimental measurements that validated the results obtained from the simulation.

We have developed a model of the system on TRSYS for simulation purposes. The diagram in Figure 5 explains the steps involved in simulating the operating parameters of the system.

Table 1 and Table 2, together with Figure 6, provide a clear and complete overview of both the experimental setup and the simulation conditions. The test bench shown in Figure 6 consists of an adsorption machine, whose characteristics are detailed in Table 1. The input parameters used for the numerical simulation are listed in Table 2.

5. Results and Discussions

In this section, we present and interpret the results obtained from both the

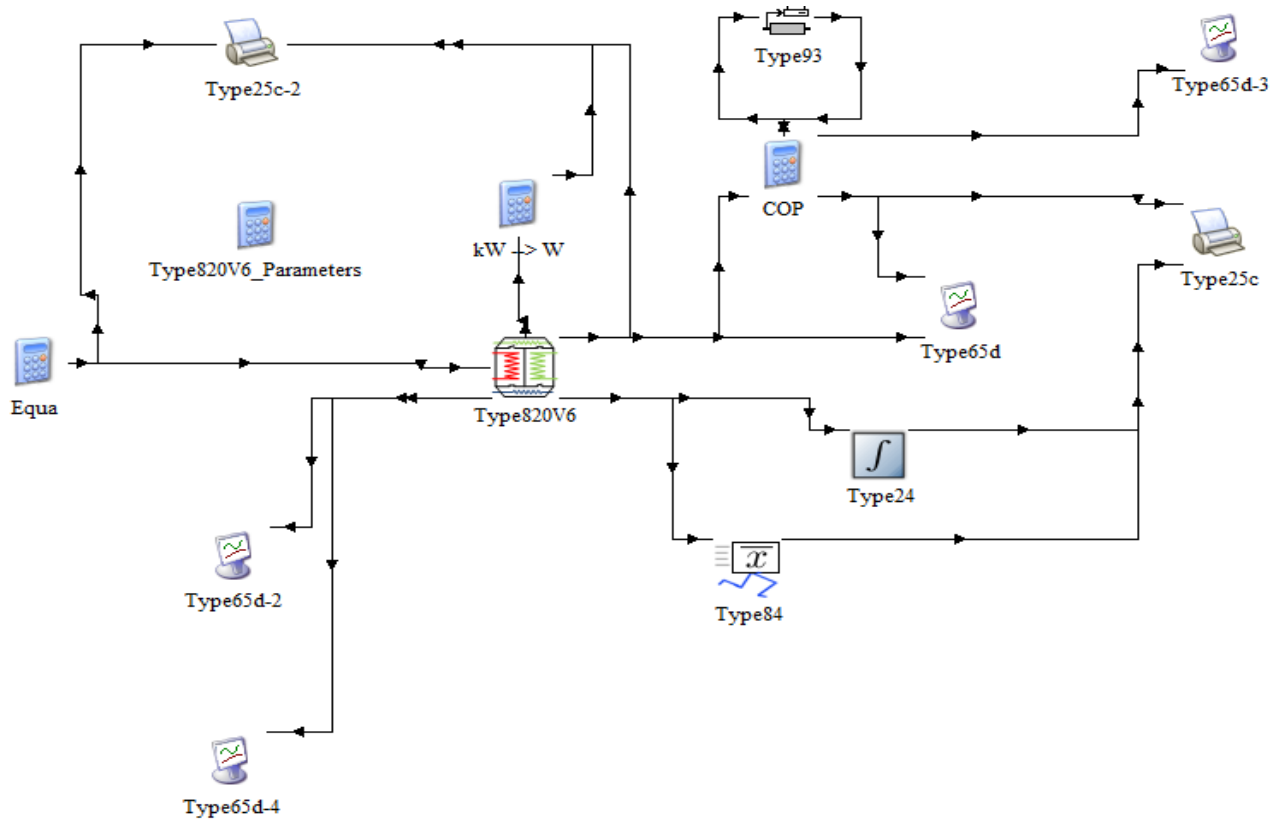

Figure 5. System model under TRNSYS.

Table 1. Main adsorber parameters and measurements.

Model	MYCOM ADR100
Rated Cooling Capacity	353 kW
Condenser/adsorber connection type	Parallel (65% adsorber, 35% condenser)
Mass recovery	No
Exchange	Yes (10 sec)
Cycle time adsorption/desorption (t_{cycle})	600 seconds

Table 2. TRNSYS input data.

Size	Value	Unit	Definition
Theat_in	65 - 90	˚C	temperature of the inlet heater or hot heat transfer fluid
Tcool_in	25 - 40	˚C	Inlet cooling temperature or cold heat transfer fluid
Tchill_in	22 - 35	˚C	temperature inlet of the heat transfer medium in the evaporator
$\dot{m}_{heat}$	100	kg/h	mass flow rate of hot heat transfer fluid
$\dot{m}_{cool}$	200	kg/h	mass flow rate of cold and condenser heat transfer fluid
$\dot{m}_{coola}$	70	kg/h	mass flow rate of cool transfer fluid
Cycle	600	s	cycle Time

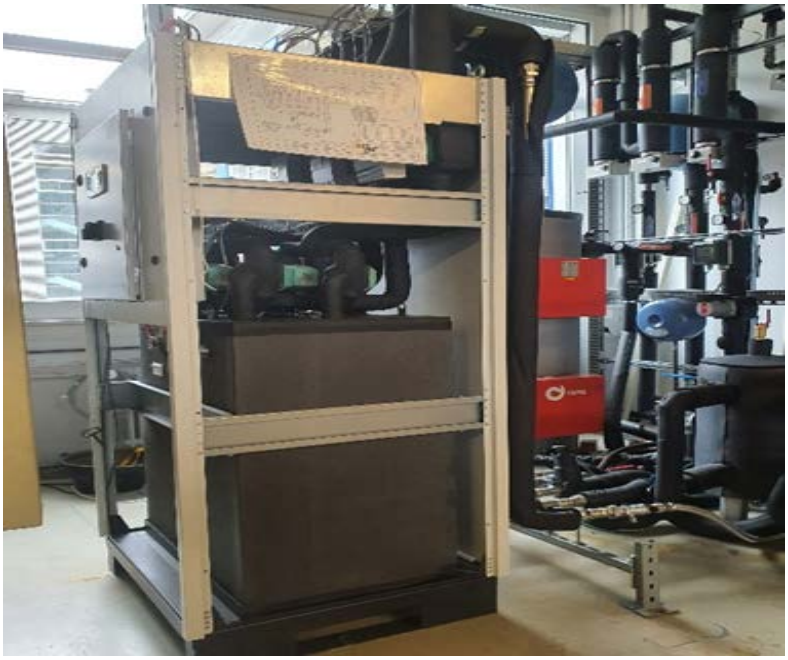

Figure 6. Test bench of a LESBAT adsorption system.

numerical simulations carried out using TRNSYS and the experimental tests conducted on the LESBAT platform. The main objective is to evaluate the thermal behavior of the adsorption refrigeration system under transient conditions and to assess the accuracy of the model by comparing it with experimental data. We focus particularly on the time evolution of temperatures and pressures in key components of the system namely, the adsorber beds, condenser, and evaporator, and analyse the system's overall performance using two key indicators: the Coefficient of Performance (COP) and the Specific Cooling Power (SCP). These results not only validate the model developed but also provide valuable insights into how variations in operating conditions, such as heating, condensation, and evaporation temperatures, affect the system's efficiency. Ultimately, this analysis lays the groundwork for optimising the design and operation of solar adsorption cooling systems tailored to hot climates, such as that of Burkina Faso.

5.1. Validation of Results

We carried out the numerical and experimental simulation of the system focusing on its operating parameters. **Figures 7-9** show the variation of the water inlet/outlet temperatures of the adsorbent beds as a function of time. The temperatures show a regular variation according to the succession of the adsorption and desorption phases for an average cycle time of about 14 minutes in the simulation and 10 min for the experiment, so there appears to be a convergence between the simulation and the experiment. The water outlet temperature of the adsorbent beds varies between the hot water inlet temperature (90˚C) which favors the driving power for desorption and the cooling water inlet temperature (25˚C) when cooling the adsorbent bed during the adsorption phase. This behaviour is

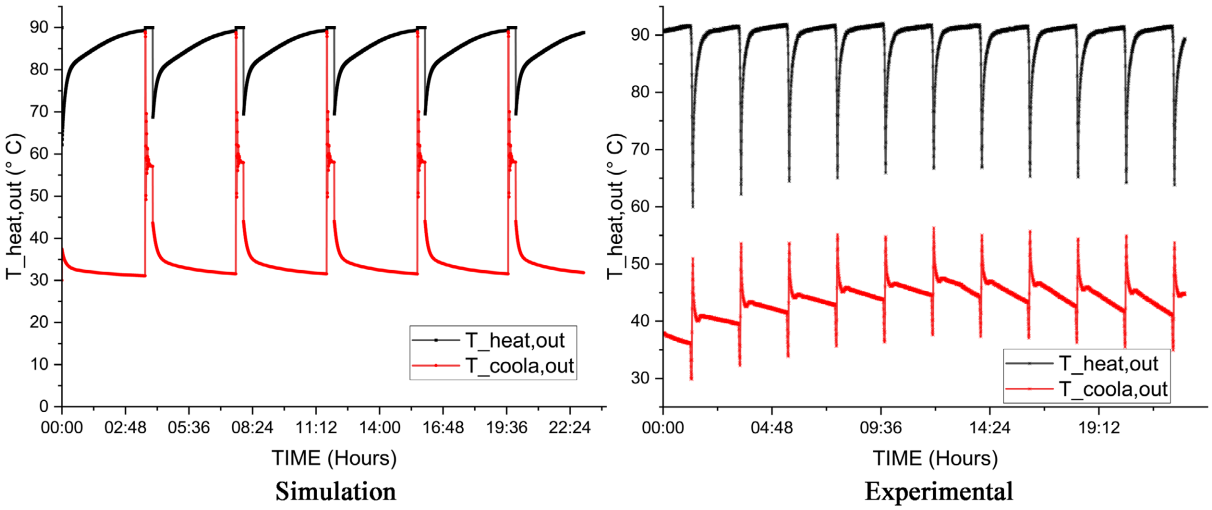

Figure 7. Temperature variation of the inlet and outlet of the condenser and evaporator.

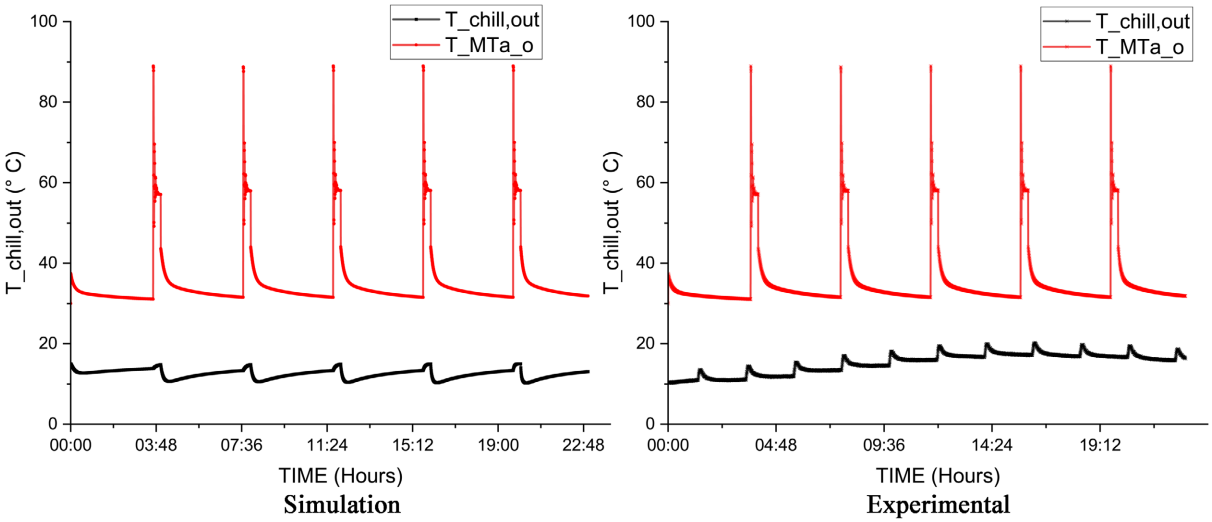

Figure 8. Temperature variation of the inlet and outlet of the condenser and evaporator.

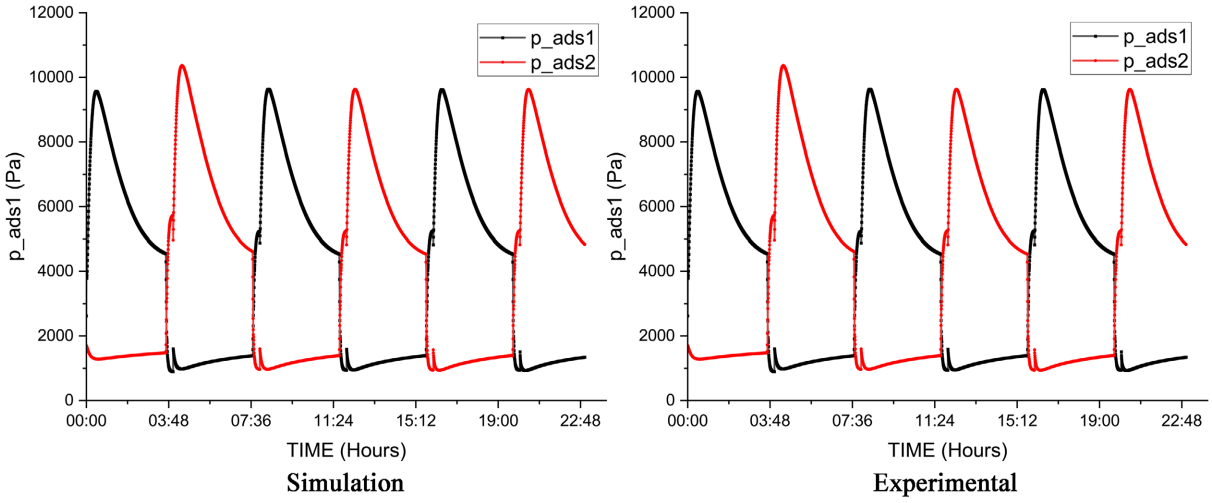

Figure 9. Pressure variation in adsorption beds.

due to the succession of adsorption/desorption phases and the role swap between the two compartments. During the desorption phase, the thermal power borrowed from the heating water decreases during the evolution of the desorption process, which is illustrated by the increase in the water outlet temperature of the desorbeur. Indeed, a large part of the heat input is accumulated by the reactor structure and by the adsorbent (silica gel) while a small part is reserved for the desorption process. When this temperature reaches its maximum value, the compartment is perfectly heated, thus allowing the water to desorption. During the adsorption phase, the thermal power dissipated in the cooling water decreases during the evolution of the adsorption process, which is illustrated by the decrease in the water outlet temperature of the desorber. Similarly, a large part of the heat rejection corresponds to the cooling of the reactor structure and the adsorbent (silica gel) while a small part is reserved for the adsorption process. Whereas when the temperature reaches its minimum value, the compartment is cooled, and the silica gel begins to adsorb water vapor.

The numerical and experimental values of the condenser's water outlet temperature vary according to the cycle and fluctuate between 25˚C and 40˚C. Figure 5 shows the numerical and experimental values of the inlet/outlet temperatures from the cold-water circuit to the evaporator. It is noticeable that the outlet temperature fluctuates between 11˚C and 13˚C with continuous cold production for a 14-minute cycle.

The following figures are obtained by numerical and experimental simulation of the variation of temperatures and pressures in the system studied. These results allow the model to be validated in order to study the performance of the system and vary the operating temperatures.

5.2. Analysis of the Performance of the System Studied

The comparison of the model with the experimental results allowed its validation in order to allow its use in simulation. Figure 10 shows the effect of the heating temperature on the performance of the machine. The machine's coefficient of performance (COP) as well as the amount of cold produced increase with the generation temperature. The performance is even better in the case of mass recovery.

The temperature of the condenser corresponds to the cooling temperature of the adsorption bed. Thus, we studied the effect of the variation of the condenser temperature on the system's COP during the day. By varying the temperature of the condenser, we also determined the variation in the amount of cold produced. Figure 11 shows the results obtained.

These figures show that the increase in the temperature of the condenser leads to a decrease in the performance of the machine.

The COP reaches its maximum value for a temperature Tc = 25˚C and after 600 s which corresponds to one cycle. However, it takes 1200 s, or two cycles, to reach the maximum value of the COP when Tc increases. However, the COP decreases when Tc increases.

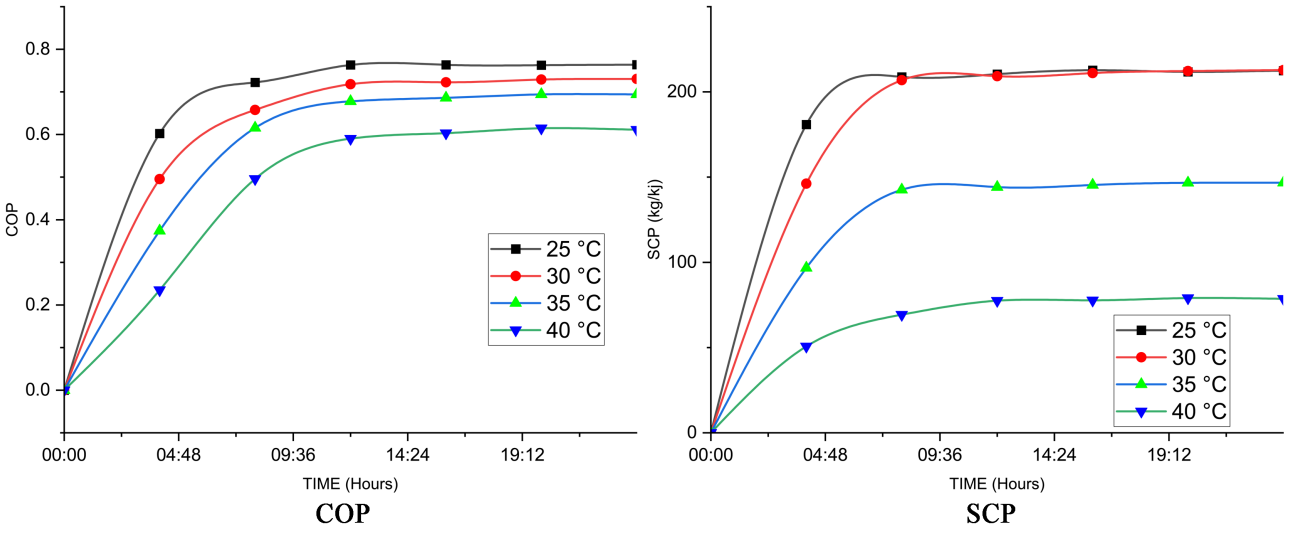

Figure 10. Variation in COP and SCP as a function of Tc.

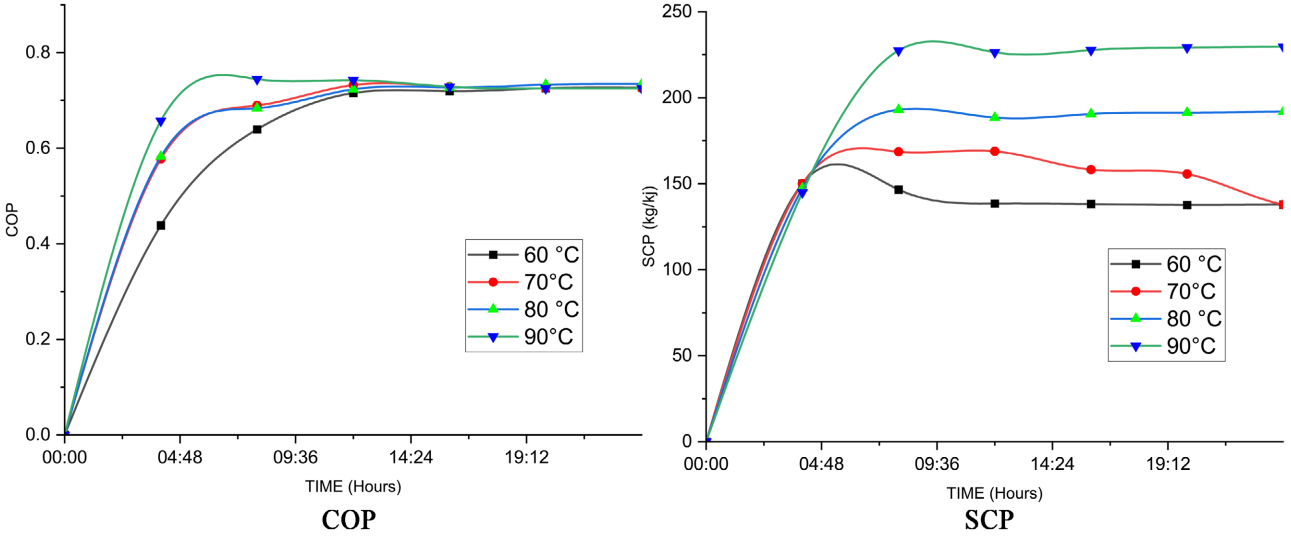

Figure 11. Variation of COP and SCP as a function of Tg.

Similarly, the SCP reaches its maximum value for a temperature Tc = 25˚C and 30˚C after 600 s, which corresponds to one cycle. However, it takes 1200 s, or two cycles, to reach the maximum value of the SCP when Tc increases. However, the SCP decreases as Tc increases.

We varied the heating temperature Tg and measured the variation in the performance of the machine and the variation in the amount of cold produced. The results are presented in **Figure 10** and **Figure 11** and highlight the variation of COP and SCP as a function of Tg temperature.

Indeed, the COP reaches its maximum value for a temperature Tg = 90˚C and after 600 s which corresponds to one cycle. However, it takes 1200 s, or two cycles, to reach the maximum value of COP when Tg decreases. We can also see that the COP decreases when Tg decreases.

We observed the variation in machine performance and the variation in the

amount of cold produced as a function of the evaporator temperature. The results are presented in Figure 12 and highlight the variation in COP and SCP as a function of temperature Te. In fact, the COP reaches its maximum value at a temperature of Te = 16˚C and after 600 seconds, which corresponds to one cycle. However, it takes 1200 seconds, or two cycles, to reach the maximum COP value when Te decreases. We also see that the COP decreases when Te decreases. Similarly, the SCP reaches its maximum value for a temperature Te = 16˚C after 1200 s, which corresponds to two cycles. However, it takes 600 s, or one cycle, to reach the maximum SCP value when Te decreases. The results show that we have one of the best system performances and the amount of cold produced when the temperature in the evaporator approaches that of the condenser.

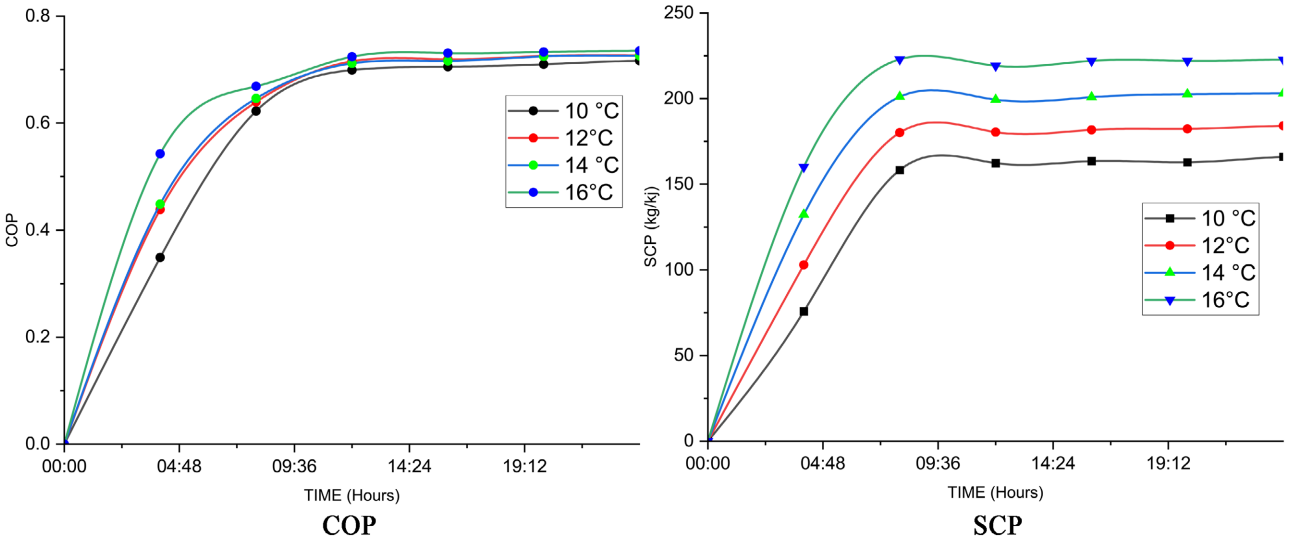

Figure 12. Variation of COP and SCP as a function of Te.

Similarly, the SCP reaches its maximum value for a temperature Tg = 90˚C after 1200 s, which corresponds to two cycles. However, it takes 600 s, or one cycle, to reach the maximum value of the SCP when Tg decreases. However, the SCP decreases as Tc increases. The results show that increasing the heating temperature increases the performance of the system and the amount of cold produced.

6. Conclusions

This work proposes a detailed modeling of a solar adsorption refrigeration system, using the silicagel-water pair. This modelling is then compared with experimental results obtained from a technological platform (LESBAT) integrating an adsorption refrigeration machine powered by a field of solar collectors.

This comparison allowed us to validate the model developed. The simulations carried out made it possible to evaluate the impact of various parameters on the overall performance of the machine, particularly with regard to heat transfer during the adsorption and regeneration processes. The conclusions of this study highlight the importance of generator and condenser temperatures on the perfor-

mance of the machine. In particular, it is recommended to increase the heating temperature (about 90˚C) while reducing the condenser temperature (keep it at about 30˚C) to improve the efficiency of the system. In addition, the analysis confirms the importance of mass transfer in the optimal operation of the machine. Finally, this model provides a solid basis for further studies aimed at optimising this type of solar adsorption refrigeration system both technically and economically.

Conflicts of Interest

The authors declare no conflicts of interest regarding the publication of this paper.

References

[1] Burkina Faso Ministry of Energy Dashboard. https://www.energie-mines.gov.bf

[2] Study on the Formulation of a Detailed Programme of Actions for the Development of the Dairy Sector within the WAEMU.

[3] Li, Z., Wang, R.Z. and Wu, J.Y. (2023) Performance Enhancement of a Solar-Driven Silica Gel-Water Adsorption Chiller by Mass Recovery Process. *Energy Conversion and Management*, **281**, Article 116810.

[4] Zhao, Y., Yu, N. and Wang, R.Z. (2022) Development and Experimental Investigation of a Compact Adsorption Chiller Using Silica Gel-Water for Solar Cooling Applications. *Applied Thermal Engineering*, **206**, Article 118086.

[5] Al Mers, A., Azzabakh, A., Mimet, A. and El Kalkha, H. (2006) Optimal Design Study of Cylindrical Finned Reactor for Solar Adsorption Cooling Machine Working with Activated Carbon-Ammonia Pair. *Applied Thermal Engineering*, **26**, 1866-1875. https://doi.org/10.1016/j.applthermaleng.2006.01.021

[6] Amadou, K. (2017) Thermal Study and Design of a Solar Adsorption Refrigerator. Ph.D. Thesis, Université Ouaga I Professeur Joseph Ki-Zerbo.

[7] Askalany, A.A., Harby, K. and Ahmed, M.S. (2021) Review on Silica Gel-Water Adsorption Cooling Systems: Performance Evaluation and Key Parameters. *Renewable Energy*, **170**, 1210-1225.

[8] Mousa, H., Kabeel, A.E. and Abdelgaied, M. (2023) Experimental Evaluation of a Solar-Powered Adsorption Refrigeration System Using Silica Gel/Water for Food Preservation in Remote Areas. *Renewable Energy*, **213**, 1381-1390.

[9] Fasfous, A., Asfar, J., Al-Salaymeh, A., Sakhrieh, A., Al-hamamre, Z., Al-bawwab, A., *et al.* (2013) Potential of Utilizing Solar Cooling in the University of Jordan. *Energy Conversion and Management*, **65**, 729-735. https://doi.org/10.1016/j.enconman.2012.01.045

[10] Mers, A.A. and Mimet, A. (2005) Numerical Study of Heat and Mass Transfer in Adsorption Porous Medium Heated by Solar Energy: Boubnov-Galerkin Method. *Heat and Mass Transfer*, **41**, 717-723. https://doi.org/10.1007/s00231-005-0618-9

[11] Bering, B.P., Dubinin, M.M. and Serpinsky, V.V. (1966) Theory of Volume Filling for Vapor Adsorption. *Journal of Colloid and Interface Science*, **21**, 378-393. https://doi.org/10.1016/0095-8522(66)90004-3

[12] Coquelet, C. (2023) Study of Refrigerants. Measurements and Modelling. Ph.D. Thesis, Ecole des Mines de Paris.

[13] Diny, M. (1996) Study of the Operation of an Adsorption Refrigeration Machine,

Modelling of Heat and Mass Transfers and Optimisation of the Machine's Operation. Ph.D. Thesis, Université Henri Poincaré, Nancy1.

[14] Passos, E., Meunier, F. and Gianola, J.C. (1986) Thermodynamic Performance Improvement of an Intermittent Solar-Powered Refrigeration Cycle Using Adsorption of Methanol on Activated Carbon. *Journal of Heat Recovery Systems*, **6**, 259-264. https://doi.org/10.1016/0198-7593(86)90010-x

[15] Sim, L.F. (2014) Numerical Modelling of a Solar Thermal Cooling System under Arid Weather Conditions. *Renewable Energy*, **67**, 186-191. https://doi.org/10.1016/j.renene.2013.11.032

[16] Poyelle, F., Guilleminot, J. and Meunier, F. (1998) Experimental Tests and Predictive Model of an Adsorptive Air Conditioning Unit. *Industrial & Engineering Chemistry Research*, **38**, 298-309. https://doi.org/10.1021/ie9802008

The Nomenclature List

Symbols	
m:	mass (kg)
$\dot{m}$:	mass flow rate (kg/h)
T:	Temperature (˚C)
t:	time (s)
Q:	amount of heat (J)
q:	specific power (W/m^2)
q^*:	adsorption capacity or maximum uptake at equilibrium (kg/kg)
q_{st}:	Isosteric heat of adsorption (KJ/kg)
h:	specific enthalpy
c_p:	calorific value (kJ/kg/˚C)
t_{ads}:	adsorption/desorption process duration (s)
t_{cycle}:	half cycle duration (s)
K_s:	fitting parameter of henry's constant
D_s:	Diffusion coefficient
R_p:	adsorbent particle average radius (0/1)
UA:	heat exchanger transmissivity (kW/K)
ϕ	flag governing adsorption/desorption in adsorber
δ:	constant fitted parameter (W/m/K)
d:	partial differential
COP:	coefficient of performance
SCP	specific cooling power

Index	
ads:	adsorber
des:	desorber
sg:	sillicagel
heat:	hot
cool:	cold
chill	chilled water
coola:	Cooling source
in:	intlet
out:	outlet
w:	liquid water,
v:	steam or water gas
cond:	condenser
eva:	evaporator
room:	room
amb:	ambient